Design of solar thermal systems utilizing pressurized hot water storage for industrial applications

G.Sudhagar[#1], Dr.V.Balaji[#2]

#1-Research Scholar, Dept of EEE, Gautam Buddh Technical University,Lucknow.

sudhagarambur@gmail.com

#2-Principal, Sapthagiri College of Engineering, Dharmapuri. Tamilnadu.

balajieee79@gmail.com

***Abstract*: A large number of industrial processes demand thermal energy in the temperature range of 80–240°C. In this temperature range, solar thermal systems have a great scope of application. However, the challenge lies in the integration of a periodic, dilute and variable solar input into a wide variety of industrial processes. Issues in the integration are selection of collectors, working fluid and sizing of components. Application specific configurations are required to be adopted and designed. Analysis presented in this paper lays an emphasis on the component sizing. The same is done by developing a design procedure for a specific configuration. The specific configuration consists of concentrating collectors, pressurized hot water storage and a load heat exchanger. The design procedure follows a methodology called design space approach. In the design space approach a mathematical model is built for generation of the design space. In the generation of the design space, design variables of concern are collector area, storage volume, solar fraction, storage mass flow rate and heat exchanger size. Design space comprises of constant solar fraction curves traced on a collector area versus storage volume diagram. Results of the design variables study demonstrate that a higher maximum storage mass flow rates and a larger heat exchanger size are desired while limiting storage temperature should be as low as possible. An economic optimization is carried out to design the overall system. In economic optimization, total annualized cost of the overall system has been minimized. The proposed methodology is demonstrated through an illustrative example. It has been shown that 23% reduction in the total system cost may be achieved as compared to the existing design. The proposed design tool offers flexibility to the designer in choosing a system configuration on the basis of desired performance and economy.**

***Keywords:* Design space; Industrial applications; Pressurized hot water storage; System integration; Solar thermal; Optimization.**

1. Introduction

A large number of industrial processes demand thermal energy in the temperature range of 80–240°C (Proctor and Morse, 1977; Kalogirou, 2003). Solar thermal flat plate collectors are not suitable for very high temperature applications. For high temperature applications, different solar concentrators may be employed. A number of solar industrial process heat systems are installed and operated on experimental basis (ESTIF, 2004). Weiss and Rommel (2005) have reported the status of the development of medium temperature solar collectors for industrial applications. The solar systems are in a developmental stage for medium temperature industrial applications and yet to achieve a full commercialization (ESTIF, 2004). The challenge lies in the integration of a periodic, dilute and variable solar input into a wide variety of industrial processes. Application- specific configurations are required to be adopted and designed. Design issues in solar industrial process heat systems involve: selection of appropriate type of collector and the working fluid, and optimal system sizing i.e., to determine the appropriate collector area, required storage volume and the si ze of the heat exchanger. As far as selection of appropriate type of collector is concerned, thermal efficiency at the desired temperature, energy yield, cost and space occupied are the deciding factors. Water, as a working fluid, is the preferred choice for low temperature applications on the basis of thermal capacity, availability, storage convenience and cost. However, for process heat applications above 100°C, water must be pressurized. Storage cost rises sharply with increasing system pressure. Commercially available mineral oils are also used for medium temperature (above 100°C) applications. However, applicability of these oils is restricted due to cost, tendency of cracking and oxidation. An important design issue in solar thermal system for industrial applications is the optimal sizing of the system i.e., appropriate sizing of the collectors, storage and heat exchanger. Different guidelines and methodologies are available to design solar thermal systems operating up to 100°C (Klein et al., 1976; Klein and Beckman, 1979; Pareira et al., 1984; Abdel-Dayem and Mohamad, 2001; Kalogirou, 2004). For systems operating above 100°C, detailed simulation programs such as TRNSYS (Klein et al., 1975) and SOLIPH (Kutscher et al., 1982) have beenapplied. However, there is a scope for developing general design guidelines for solar industrial process heat systems for medium temperature applications (Clark, 1982; Eskin, 2000; Weiss, 2003). In this paper, a methodology is developed to design and optimize a solar thermal system with pressurized water for

medium temperature industrial applications. The analysis is carried out by applying the design space concept (Kulkarni et al., 2007). The design space is represented by tracing constant solar fraction lines on a collector area vs. storage volume diagram for a specified load. In this approach, all possible and feasible designs of a solar water heating system can be identified. Investigations in this paper comprise a design variable study and system optimization. Effects of different design variables on the collector area; storage volume and system performance are studied with the help of identified design space. The study is commenced by fixing the variables one by one. To consider the combined effects of additional design variables such as heat exchanger size and maximum storage operating pressure, economic optimization is needed. A global economic optimum is obtained for the given configuration. The proposed procedure is demonstrated through an illustrative case study of integrating solar concentrator with pressurized hot water storage to deliver 45000 l of hot water to pasteurize 30 000 l of milk per day. Compared to the existing system, the optimum design, obtained usingthe proposed methodology, and offers 23% reduction in the total annualized cost.

2. The design space

It is a approach Design space, introduced by Kulkarni et al. (2007) is the region bounded by constant solar fraction curves traced on the collector area vs. storage volume diagram. Design space approach involves identification of the entire design space i.e., all the feasible system sizes. The procedure of design space generation is reviewed briefly in this section and illustrated with the help of an example. Schematic of a flat plate solar water heating system is shown in Fig. 1. For such a system, energy balance for the well mixed storage tank can be expressed as a differential equation. Change in the internal energy of the storage tank is equal to the energy interactions taking place over a time step. The energy interactions are solar input, demand met and the storage heat losses: In estimating storage tank heat losses, surface area of the storage tank is assumed to be related to the storage volume by following relation, assuming equal height to diameter ratio (Kulkarni et al., 2007):

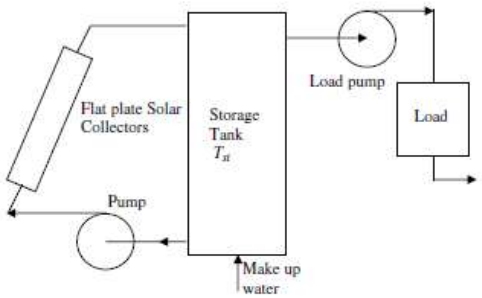

Fig.1. Schematic of a solar water heating system.

assumed that change in the thermal energy of the storage over the time horizon (a day, a month or a year) is zero: By varying the collector area and the storage volume, different feasible designs may be obtained. For illustration, a case of unity solar fraction is described. Unity solar fraction suggests that the entire thermal demand has to be met by the solar energy.

For satisfying the entire thermal demand, storage tank temperature during the time of the demand must be greater than the desired load temperature: An acceptable design must satisfy these constraints. For a specified load, all possible combinations of collector area and storage volume that satisfy these two constraints define the design space. Generation of the design space is demonstrated through an example. A single day (15th April) is chosen for illustration. Monthly mean values of hourly solar radiation (Mani, 1981) are adopted for this example. The time step t is 3600 s and time horizon is a single day. The system parameters are given in Table 1. Fig. 2 shows the storage temperature profile with a typical collector area and storage volume combination (Ac = 90 m2 and Vst = 3.7 m3). Limiting storage temperature constraint and the hot water demand profile are also shown in Fig. 2. The limiting storage temperature constraint is 100°C while the load temperature constraint is 60°C. The storage temperature profile is in between these two constraints (Fig. 2). This is a feasible design for unity solar fraction. The combinations of Ac and Vst are varied to obtain all the feasible designs for unity solar fraction. Combination of the collector area and the storage volume that satisfy these constraints are identified and illustrated in Fig. 3. The region inside these curves represents all possible design combinations that satisfy the unity solar fraction. This region represents the design space for unity solar fraction for the example. From Fig. 3, it may be noted that the point ‘a’ represents a system with the lowest possible storage volume requirement. Point ‘a’ represents 2.6 m3 of storage volume and 111 m2 of collector area. Any reduction in storage volume will result in boiling of water in the storage tank. Point ‘m’ in Fig. 3 indicates a

minimum collector area design. The design occurs at a collector area of 76 m2 and storage volume of 28 m3. Any decrease in the collector area from 'm' will not meet the desired hot water demand. It may also be noted that there exists a minimum as well as a maximum storage volume for a given collector area. For example, a constant collector area line (Ac = 111 m2) in Fig. 3 intersects the limiting curves at 'a' and 'b'. Point 'a' indicates a minimum limit on storage volume of 2.6 m3, while point 'b' indicates a maximum limit of 1227.2 m3. Beyond point 'b', thermal losses from the storage tank will dominate resulting into a loss of solar fraction. Similarly, there exists a minimum as well as a maximum collector area for a given storage volume. It is illustrated in Fig. 3 through points 'm' and 'o'. The line segment 'ma' in Fig. 3 signifies the Pareto optimality curve. The region bounded by the limiting curves includes all feasible designs of the system and is called the design space (Kulkarni et al., 2007). Similar to the above procedure, the design space can be identified by tracing constant solar fraction lines for other solar fractions. Any objective function involving the capital and the operating costs of the system may be chosen for optimization of the overall system A more elaborate treatment of design space is given by Kulkarni et al. (2007). Application of the design space approach has been demonstrated for solar thermal system operating up to 100°C. A large number of industrial and commercial applications demand solar thermal energy beyond 100°C. Utility of the design space methodology is therefore, improved and extended for systems operating beyond 100°C. 3. The design space for pressurized water storage in this section, the concept of design space is improved and extended to a solar thermal system intended for Indus trial application beyond 100°C. 3.1. System configuration The general configuration of a solar thermal system supplying hot water beyond 100°C is shown in Fig. 4. The general system comprises of a concentrating collector, a pressurized hot water storage tank, a load heat exchanger and an auxiliary heater. The beam solar radiation is converted into useful heat by the concentrating collector.

Water from the storage tank is circulated through the absorber tubes of the receiver. Water absorbs the heat and is returned back to the storage tank. Heat is stored in the form of pressurized hot water. When heat is demanded by the process, hot water is pumped to the heat exchanger at a rate of mst. Hot water at Thi from the storage tank is circulated through the heat exchanger. In the heat exchanger, heat is transferred to the cold stream. Water returns to the storage tank at a lower temperature of Tho. The cold process stream is pumped at a constant flow rate of mc. A minimum cold stream outlet temperature (Tco,min) is desired to meet the entire demand. This limit can be determined on the basis of the demand and the cold stream flow rate. Actual cold stream outlet temperature (Tco) depends on the storage temperature Tst. Auxiliary heater is placed in the cold stream circuit in series with the heat exchanger. If Tco < Tco, min, auxiliary heater is switched on and the cold stream is further heated to the desired temperature.

The design variables for this generalized system are

- Collector area (Ac),
- storage volume (Vst),
- solar fraction (F),
- maximum storage mass flow rate (mst,max),
- heat exchanger sizing parameter (UA) and
- limiting storage temperature (Tst,max).

The limiting storage temperature determines the maximum operating pressure of the system and the thickness of the storage tank. For simplification, it is assumed that the type of heat exchanger and its size may be characterized and selected on the basis of UA product. UA product represents the output of a heat exchanger for a unit logarithmic temperature difference (LMTD). Design procedure proposed here uses UA product as a heat exchanger sizing parameter. It may be noted that Eq. (9) represents a

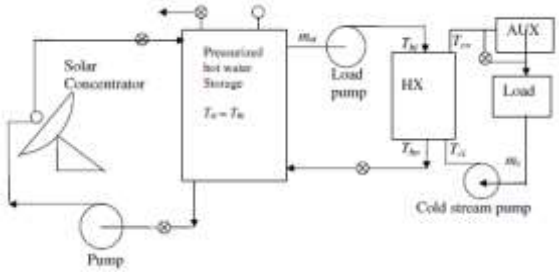

Fig.4. Schematic of a solar industrial process heat configuration.

characteristic equation for a solar collector. For high temperature applications and for concentrating collectors, this may not always be suitable. For such systems, a second or higher order characteristic equation may be more suitable. For more accurate results, a non-linear characteristic equation should be used instead of (9). The proposed methodology is independent of the nature of the characteristic equation. However, for the system, for which the methodology is demonstrated, it has been observed that an accurate non-linear characteristic equation does not improve the system sizing significantly (Kulkarni, 2008). D hot stream temperature Thi is the storage temperature Tst. Number of transfer units (N), heat capacity flow rate ratio (R) and cold or hot fluid temperature effectiveness (P) are defined as follows: Computation begins with the assumption of initial storage temperature (Tsti), storage

flow rate (mst) and heat exchanger sizing parameter (UA). With these parameters known, values of N and R can be calculated using Eqs. (13) and (14). For simplicity, a counter flow heat exchanger is assumed. With hot stream effectiveness P known, hot stream outlet temperature The minimum cold process stream outlet temperature (Tco,min) needed to fulfill the complete demand can be determined as T By knowing the hot stream outlet temperature, solar contribution to the load during a time step may be determined. In Eq. (19), desired load (QL) over a time horizon (a day) and duration of load in nL time steps (number of hours) is specified. The load is assumed to be uniformly distributed over the time steps. Cold stream mass flow rate (mc) and inlet temperature (Tci) are assumed to be constant in this analysis. No auxiliary energy will be required if Tco P Tco,min. In all the cases, hot stream flow rate is controlled in such away that cold stream outlet temperature does not exceed Tco, min. This ensures effective utilization of the solar energy. The final storage temperature at the end of a time step will be the initial temperature for the next time step. Storage temperature profile over a day is thus, obtained.

The maximum storage temperature (Tst,max) observed in a day is identified. In this model, the maximum storage operating pressure is the saturation pressure of water corresponding to the maximum storage temperature. The correlation proposed by Chopey (2004) is used to determine the saturation pressure of water corresponding to the maximum storage temperature. It is assumed that there is no change in the internal energy of the storage over the time horizon (a day, a month or a year). Equations described above are utilized to study the effect of different variables on the system design and performance.

3.3. Effect of different design variables

In this section, effects of various design variables on the overall system design and operations are investigated. Effects of the maximum storage mass flow rate, heat exchanger size and the limiting storage temperature on the system design are studied. In each case, the design space for unity solar fraction is generated and it is illustrated with an example of milk pasteurizing process. The load has a daily demand of 45000 l of hot water for pasteurizing 30000 l of milk per day. Load details and other input data are given in Table 2. The configuration uses concentrating collector that operates on the beam solar radiation. In the major part of India, July, August and September are monsoon months. During monsoon months almost no beam solar radiation is available. Considering this fact, monthly average of hourly normal beam radiation data (Mani, 1981) neglecting these three months is considered. A nine month average is calculated to represent a single day.

Fig. 5 shows the variation of a nine month hourly average normal beam radiation over time. Analysis presented in the following sections makes use of a nine month average of beam solar radiation intensity. Ambient data is adopted on the similar lines. Time step in all the foregoing analysis is 3600 s while time horizon is single day. It may be noted that the proposed methodology is not restricted to these assumptions.

3.3.1. Effect of maximum storage mass flow rate

Effect of storage mass flow rate on the system design is investigated. Storage mass flow rates are varied from 2 kg/s to 10 kg/s. Other system parameters such as heat exchanger UA value and limiting storage temperature, etc. are kept constant. Results are shown in Table 3. Average collector efficiency and average heat exchanger effectiveness are calculated using Eqs. (25) and (16), respectively. From Table 3 it may be observed that the average storage temperature during the load period, the collector efficiency and the solar fraction changes only slightly. However, the average heat exchanger effectiveness reduces with increasing storage mass flow rate. Design spaces for unity solar fraction at different storage mass flow rates are shown in Fig. 6. The characteristics are drawn at a constant heat exchanger UA value of 6000 W/°C and the limiting storage temperature of 160°C. Designs with the minimum collector area as well as the minimum storage

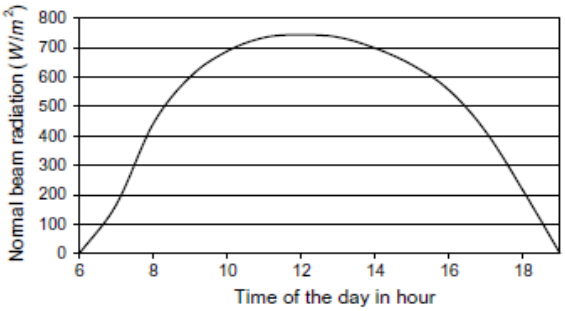

Fig.5. Average daily direct normal radiation used for the illustrative example.

Table 2
Input data for pressurized hot water storage system example

Location	A dairy plant at Pune, India
Load	Pasteurization load, $\dot{Q}_L$ = 1.88 GJ/day (30000 LPD of milk) Duration: Five hours in t_L 19 a.m. to 0230 p.m., uniform Cold stream mass flow rate m_c = 3.125 kg/s, inlet temperature T_{ci} = 85 °C, outlet temperature $T_{co,min}$ = 95 °C
Collector	Parabolic collector with two axis tracking (η_0 = 0) $F_R(\tau\alpha)$ = 0.6 and $F_R U_L$ = 1.2 W/m² K (Kalogirou, 2004) Working fluid: Water
Storage	Storage fluid: Water, pressurized Tank Material: Carbon steel C21, density 7800 kg/m³ Cylindrical, self-stand, always full, with $(H/D)_s$ = 2.6 Tensile stress for tank material, σ_{ts} = 50 MPa (PSG, 1988) Factor of safety for pressure vessel design, f_s (Brownell and Young, 1959) Design stress = 20 MPa Insulation thickness, t_{ins} = 152.4 mm Insulation: Glass wool (k_{ins} = 0.06 W/m K)
Heat exchanger	Counter flow type $C_{pc} = C_{ph}$ = 4400 J/kg K

Table 3
Effect of maximum storage mass flow rate on the system performance at a fixed system size of Ac = 180 m2, Vst = 4m3, UA = 6000 W/°C, Tst,max = 160°C

Maximum storage mass flow rate, kg/s	Average storage temperature during load period, °C	Average collector efficiency	Average HX effectiveness during load period	Solar fraction
2	114.38	39.72	63.09	0.8859
3	112.62	40.61	56.14	0.895
4	111.9	40.14	52.35	0.8965
5	111.61	40.2	50.63	0.8978
6	111.41	40.25	49.44	0.8988
7	111.27	40.28	48.58	0.8995
8	111.16	40.3	47.91	0.9
10	111.02	40.33	46.97	0.9008

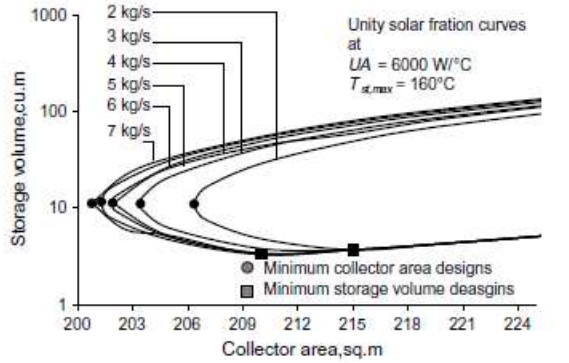

Fig.6. Design spaces at unity solar fraction for different maximum storage mass flow rates.

volume, corresponding to the unity solar fraction for different storage mass flow rates, are highlighted in Fig. 6. It may be noted that the storage mass flow rate does not have a significant impact on the storage volume. However, the minimum collector area requirement decreases significantly with increasing maximum storage flow rate. Higher values of storage mass flow rates are therefore, desired. It may be noted that the higher mass flow rate of the storage water requires more electrical power required to pump it through the heat exchanger. Appropriate hydraulic analysis may be performed to select the maximum storage mass flow rate.

3.3.2. Effect of heat exchanger size (UA)

At a fixed system size, Table 4 shows the effect of heat exchanger UA value on the system performance. As heat exchanger UA value increases the heat exchanger effectiveness increases and the average storage temperature during load decreases. This results in an improvement in the solar fraction and a reduction in the minimum collector area requirement (Fig. 7). In Fig. 7, the effect of heat exchanger size, on the design space for unity solar fraction is revealed. The limiting storage temperature lines for different heat exchanger sizes are separately drawn. The minimum storage volume requirements i.e., the intersections of the constant unity solar fraction curves with the limiting storage temperature lines are depicted by points 'a' to 'f'. The minimum collector area requirements are represented by points

Table 4
Effect of heat exchanger size on system performance at a fixed system size of Ac = 180 m2, Vst = 4 m3, mst,max = 3 kg/s and Tst,max = 160 °C

UA, W/°C	Average storage temperature during load period, °C	Average heat exchanger effectiveness during load period	Solar fraction
2000	136	15.2	0.78
2600	127.8	23.7	0.82
3000	123.8	28.1	0.84
4000	118.7	41.5	0.86
6000	112.6	56.1	0.89
8000	110.1	67.6	0.90
10000	108.6	74.8	0.91

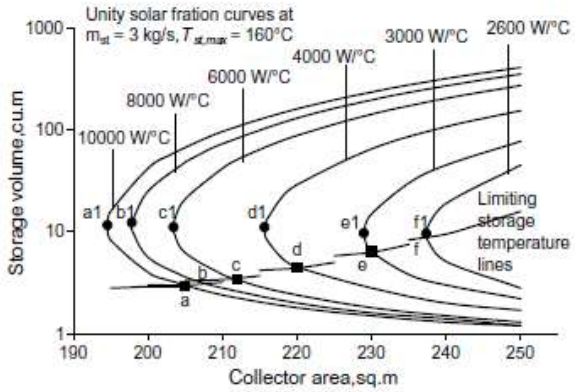

Fig. 7. Effect of heat exchanger sizing parameter on the design spaces at unity solar fractions at Tst,max = 160°C, mst,max = 3 kg/s.

'a1' to 'f1'. With a decrease in UA value (heat exchanger size), the minimum collector area requirement as well as the minimum storage volume requirement increases. The Pareto optimal region is the portion of the constant solar fraction curve connecting the minimum collector area and the minimum storage volume. A suitable economic criterion may be applied to obtain an optimum design. With a decrease in heat exchanger UA value, Pareto optimal curve begins to shrink. For this example, at an UA value of 2600 W/°C, the point denoting the minimum collector area requirement and the point denoting the minimum storage volume requirement, coincide and the Pareto optimal curve shrinks to a point (point 'f' in Fig. 7). For designing a system with heat exchanger UA values less than 2600 W/°C, economic optimization is not required, as the Pareto optimal region is represented by a single point. A larger heat exchanger may be preferred as the minimum collector area requirement and the minimum storage volume requirement both decreases simultaneously. However, a large heat exchanger incurs a higher capital cost. Economic optimization of the overall system may be carried out to choose the appropriate heat exchanger size.

3.3.3. Effect of limiting storage temperature

The limiting temperature of the storage tank (Tst,max) signifies the operating pressure of the system. With an increase in Tst,max, the operating pressure of the system increases and thereby, thickness of the storage tank and associated piping system increases. This results in an increase in the capital cost of the overall system. Fig. 8 shows design space at unity solar fraction at various limiting storage temperatures. The characteristics are drawn at a constant maximum storage mass flow rate of 3 kg/s and heat exchanger UA value of 6000 W/°C. The limiting storage temperature lines for different maximum allowable storage temperature are shown separately in Fig. 8. The minimum storage volume requirement reduces significantly with increasing limiting storage temperature. For the example, required minimum storage volumes correspond to different limiting storage temperatures are highlighted by points 'a' to 'e' in Fig. 8. It may be noted that the minimum collector area requirement does not vary significantly if the maximum storage temperature is beyond a particular value. For the example, it has been noted that below 130°C of the limiting storage temperature, the sizing curve shrinksin to a point. From the above study, it may be noted that the maximum storage mass flow rate, heat exchanger size, and the limiting storage temperature influences the minimum collector area requirement as well as the minimum storage volume requirement. In other words, the design space gets affected by these variables. To capture the effect of these variables simultaneously on the design space, an optimization based methodology is proposed.

3.4. Design space through system optimization

A methodology to generate the design space of the system considering simultaneous variation of different design parameters is discussed here. It may be noted that for a given collector area there exist a maximum and a minimum storage volume in the design space. Based on this observation, a methodology is followed to generate the design space where different design variables are varied simultaneously. The maximum and the minimum allowable storage volumes are searched subject to different constraints. These objectives (minimization and maximization of the storage volume) are optimized separately by varying heat exchanger size and the maximum storage flow rate subject to a given collector area and solar fraction. For a fixed solar fraction, by varying the collector area, the loci of the maximum and the minimum allowable storage volumes are plotted on the collector area vs. storage volume diagram to obtain the design space of the system. Input parameters include solar radiation data, daily thermal demand, desired solar fraction, collector characteristics, storage parameters, working fluid properties etc. During optimization, to limit the search space and to have a physical significance of the result, suitable range for each variable has been incorporated.

A limit on the maximum storage temperature is kept for the safety purpose. The limit depends on collector type, nature of demand and storage cost. At any instant of time storage temperature should not exceed the limiting specified value. As the storage temperature decreases, the duty of the auxiliary heater has to be increased to fulfill the demand. There is a practical limit on the provision of auxiliary heater capacity. It is not beneficial to operate the system at very low storage temperatures. A lower limit on storage temperature is therefore, provided. The cold process stream inlet temperature should ideally serve as a lower limit. Due to finite size of the heat exchanger, a certain temperature difference (dT) is maintained. At any instant of time, storage temperature should be above the minimum specified limit. Similarly, the minimum and the maximum size constraints are put on the heat exchanger size: On the hot stream side, it is assumed that there is a minimum temperature difference between the inlet and the outlet temperature. Corresponding to this minimum temperature difference, a maximum storage flow rate exists:

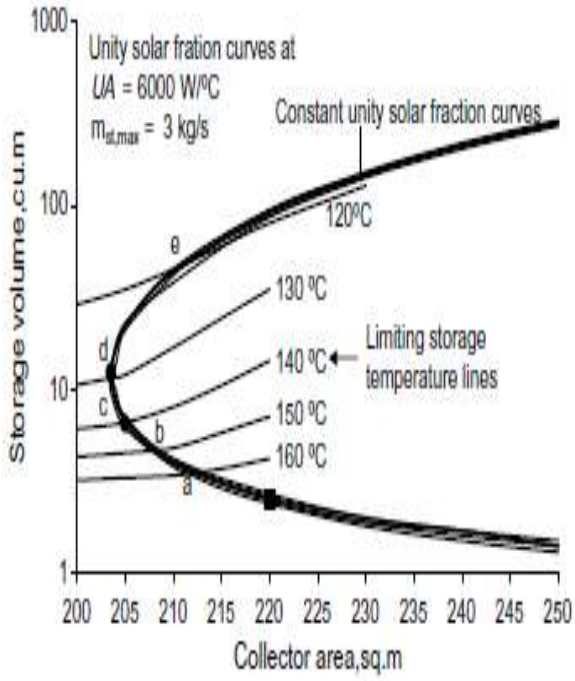

Fig.8. Effect of maximum storage temperature on the design space for unity solar fraction at UA = 6000 W/°C and mst, max = 3 kg/s.

Table 5
Constraints in the optimization formulation

Description of the constraint	Value
Limiting storage temperature constraint, $T_{st,max}$	200 °C
Minimum cold stream inlet temperature, T_{co}	85 °C
Minimum storage temperature, $T_{st,min}$	90 °C
Maximum storage flow rate, $m_{s,max}$	6 kg/s
Maximum UA value, $UA_{,max}$	8000 W/°C
Minimum UA value, $UA_{,max}$	2000 W/°C

The above model is optimized for the minimum and the maximum storage volume. The proposed procedure for generation of the design space is demonstrated through the previous example. Limiting values of different constraints are tabulated in Table 5. The design space generated is shown in Fig. 9. Curves in Fig. 9 represent constant solar fractions in the range of 0.6–1. In each case, the minimum collector area and the minimum storage volume points are highlighted. The design space portrays variation between the collector area and the storage volume at different solar fractions. The effects of three variables on the collector area, the storage volume and the solar fraction are accounted. It may be noted that the design space does not exhibit the effect of these variables on the economic design on the overall system. As discussed earlier, it has been observed that a larger heat exchanger is desired. However, a larger heat exchanger incurs a higher capital cost. Lower halves of the constant solar fraction curves in Fig. 9 are obtained by minimizing the storage volumes. These designs represent heat exchanger sizes that designate a minimum storage volume and not necessarily the minimum system cost. Heat exchanger size must be optimized on the economic basis rather than minimum storage volume requirement. Similarly the effect of maximum storage temperature on the economic optimization of the overall system is not visible on the design space. Maximum storage temperature decides the maximum storage operating pressure and storage tank thickness. A higher storage temperature indicates a lower storage volume and associated reduction in the capital cost. Higher storage temperature also increases tank thickness increasing the capital cost. The design space tends to demonstrate maximum tank thickness while minimizing the storage volume. An economic trade off is possible between storage tank volume and tank thickness (weight). The reason being, additional variables influence the system size, besides collector area and storage volume. To account for the effect of additional variables such as heat exchanger size and maximum storage temperature, economic optimization is carried out. This highlights the difference between the design space for simple flat plate solar thermal system and that for a concentrator solar thermal system with pressurized hot water storage. Because of additional variables, the design space does not incorporate the Pareto optimal region for a solar thermal system with pressurized hot water storage.

4. Economic optimization of the overall system

For economic optimization of a solar thermal system, different objective functions such as total annual cost (Kulkarni et al., 2007), annualized life cycle cost (Hawlader et al., 1987), life cycle savings (Gordon and Rabl, 1982), payback period (Michelson, 1982), internal rate of return (Gordon and Rabl, 1982) etc. have been considered. In this paper, total annualized cost of the system (TAC) has been used as an objective function. The total annualized cost of the system comprises of the annualized capital cost, annual repair and maintenance costs of the overall system. Cost coefficients used for this study are reported in Table 6, based on the existing market trends in India. In the design of chosen configuration, storage tank thickness varies with the maximum storage temperature as well as storage volume. The cost coefficient of storage volume is therefore, mentioned in terms of cost per unit storage volume and unit tank thickness. Total annualized cost of the system is given as

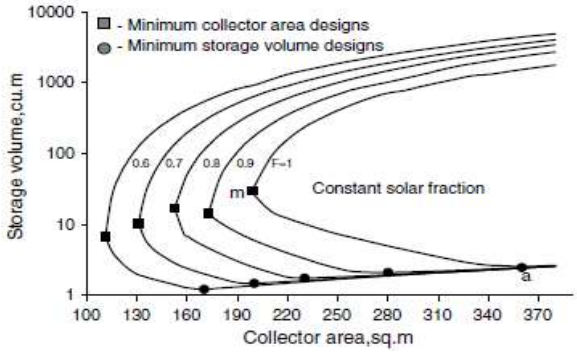

Fig.9. Entire design space with optimized storage volume.

Table 6
Economic parameters adopted for optimization

Discount rate, r%	10.75
Life of collectors and storage, n years	15
Life of heat exchanger, years	5
Life of auxiliary heater, n_{aux} years	10
Collector cost coefficient, C_c US$/m^2	333
Storage tank material cost US$/kg	1.1
Storage tank cost coefficient per m^3 US$/mm of wall thickness	59
Tank insulation price, C_{ins} US$/m^2	3 (for a slab thickness of 25.4 mm)
Heat exchanger cost coefficient, US$/kW/°C	555
Cost coefficient of hot water generator, C_R, US$/kW	89
Fuel price (LDO), C_F US$/kg	0.9
Burner efficiency	75%

Table 7
Economic optimum designs at different solar fractions

Solar fraction	1.00	0.90	**0.87**	0.80	0.70	0.60	0.50
Collector area, m^2	207	176	**170**	156	136	116	97
Storage volume, m^3	17	12	**11**	8	5	5	4
Heat exchanger UA value, W/°C	8000	6226	**5840**	5117	4403	3740	3002
Maximum storage temperature, °C	119	119	**121**	123	127	127	127
Maximum operating pressure, bar	2	2	**2**	2	2	2	2
Tank thickness, mm	31	29	**28**	28	27	26	24
Total cost, US$/y	14763	14237	**14180**	14251	14555	14988	15248
System capital cost, US$/y	14763	12704	**12187**	11226	9998	8839	7687
Operating (fuel) cost, US$/y	0	1533	**1993**	3025	4557	6149	7561

Annual repair and maintenance cost of the collector and storage is taken as 2% of the capital cost while that of the heat exchanger is taken as 3% of its capital costs. For the case study, the auxiliary heater operates on light diesel oil. Auxiliary heater rating Ra is determined from the period of the maximum auxiliary energy demand. The mathematical model described in Section 3.2 is transformed into an economic optimization formulation. All the input parameters and constraints remain the same as in Tables 2 and 5 respectively. The objective function is minimization of total cost by varying collector area, storage volume, heat exchanger UA value and storage mass flow rates within a specified range and results are shown in Table 7. It may be observed from Table 7 that reduction in the solar fraction reduces the collector area, the storage volume, and the heat exchanger size requirement. There is a marginal increase in the maximum storage temperature (and corresponding operating pressure) with a reduction in solar fraction. It is interesting to note that the tank thickness decreases even if there is an increase in the storage temperature. The decrease in tank thickness is attributed to a reduction in the storage volume (22). As the solar fraction decreases, capital cost decreases while operating cost increases. A tradeoff between the capital and the operating costs yields a solar fraction with the minimum total cost of the system. Fig. 10 shows the variation of total cost with solar fraction. For the given constraints, the global economic optimum is observed at a total cost of US$14180/y and at a solar fraction of 0.87. A comparison of the optimum design with the existing design is shown in Table 8. In actual practice, commercial concentrating collectors are available only in discrete sizes. The type of concentrating collector used for this study is available at a fixed size of 160 m2.

The entire economic optimization is performed with a fixed collector size of 160 m2. Table 8 also shows an optimized design with a fixed collector area of 160 m2. Existing design consists of 160 m2 of collector area, 5 m3storage volume, heat exchanger UA value of 3500 W/°C and the storage tank thickness of 160 mm. The existing design gives a solar fraction of 0.78 and the annualized system cost of

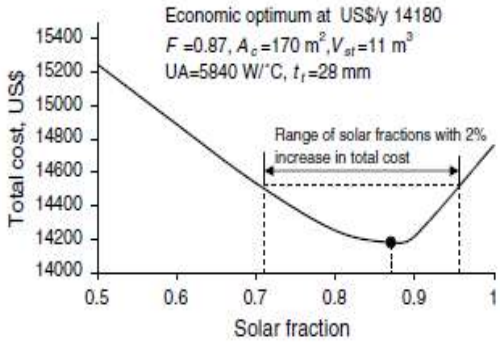

Fig.10. Variation of total cost with solar fraction.

Table 8
Comparison of global economic optimum with existing design

	Optimum design	Existing design	Optimized design with fixed collector area
Solar fraction	0.87	0.78	0.82
Total cost, US$/y	14180	18956	14213
Solar system Capital cost, US$/y	8557	10455	7125
Auxiliary heater Capital cost, US$/y	3630	4240	4427
Operating (fuel) cost	1993	3303	2661
Collector area, m^2	170	160	160
Storage volume, m^3	11	5	9
Heat exchanger UA value, W/°C	5840	3500	5572
Maximum storage temperature, °C	121	200	122
Maximum operating pressure, bar	2	16.00	2.1
Tank thickness, mm	28	160	27

US$/y 18956. For the given constraints, the optimum design exhibits a better economic benefit and performance than the existing design with and without a given collector area. The global optimum design depicts a 12% gain in the solar fraction at the cost of 21% increase in the solar capital cost as compared to the existing design. An overall benefit of 25% is expected in the total annualized cost for the global optimum design. As compared to the existing design, there is an increase in the collector area of 6%, an increase in storage volume by 120% and an increase in the heat exchanger size by 67%. However, there is a 40% reduction in the maximum storage temperature and it brings down the maximum operating pressure by 88% and the tank thickness by 83%. Overall capital cost decreases substantially with a reduction in the maximum operating pressure of the storage tank. There are also a 23% reduction in auxiliary heater capital and

41% reduction in operating cost. Designing the system with a lower limiting storage temperature thus, improves the economic advantage. The optimized design with a fixed collector area of 160 m2 shows no substantial change from the global optimum design. There is a 2% increase in the total annualized cost of the fixed collector area design. The increase is attributed to a 21% increase in the auxiliary heater capital and a 33.5% increase in the operating cost. In comparison of fixed collector area design with the existing design demonstrates that there is a 21% saving in the operating cost. Storage temperature profile with the global optimum system design is shown in Fig. 11. Milk pasteurization load occurs between 10 a.m. and 2 p.m. In the morning hours, up to 10 a.m. there is insolation but no demand. These raises the storage temperature to 120°C. Withdrawal of heat during demand decreases the storage temperature to a minimum of 103°C at 2 p.m. Beyond 2 p.m. storage temperature steadily lifts up till sunshine is available upto 5 p.m. From Fig. 10, it may be noted that the TAC curve does not change significantly near the global optimum. Due to uncertainties associated with system parameters, solar isolation, cost data, etc. a globally optimum value may not necessarily provide a meaningful result in actual practice. Similar observations were reported by Shenoy et al. (1998) in designing and optimizing heat exchanger networks. A 2% margin is allowed for the minimum total annualized cost. The lower and the upper limits of solar fractions corresponding to a 2% increase in the minimum total annualized cost are shown in Fig. 10. The limits of solar fractions are observed to be 0.71 and 0.98 respectively. The corresponding costs and system parameters are shown in Table 9. At the lower limit of solar fraction (F = 0.71), the system configuration requires 26% lower capital investment as compared to the upper limit.

Solar fraction	0.71	0.978
Total cost, US$/y	14471	14461
System capital cost, US$/y	10085	14126
Operating (fuel) cost	4386	334
Collector area, m^2	138	200
Storage volume, m^3	6	14
Heat exchanger UA value, W/°C	4554	7448
Maximum storage temperature, °C	127	121
Maximum operating pressure, bar	2	2
Tank thickness, mm	27	30

Amount of auxiliary energy needed is nearly 12 times higher. On the other hand, the upper limit of solar fraction (F = 0.98) implies a system configuration with higher capital investment and lower operating cost. Based on the available cash flow for investment, an appropriate system configuration may be chosen for the process heat application. The design procedure is illustrated using a single day analysis. The system can be designed more precisely by incorporating the annual radiation data in a dedicated Optimizer tool. It may be noted that the nine-month average beam normal radiation data are used for the single day analysis. The results obtained using a single day analysis matches with the system data is a

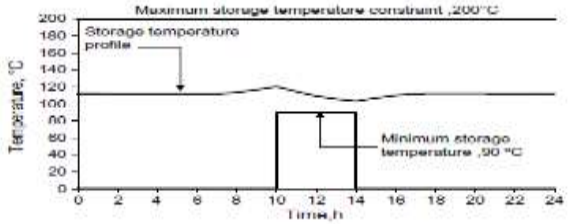

Fig.11. Storage temperature profile with optimum system size, Ac = 148 m2, Vst = 7 m3.

obtained from the field (Kulkarni, 2008). The methodology has been successful in application to a specific configuration of industrial process heating. However, the same can be effectively applied in the design and optimization of a variety of configurations.

5. Conclusions

Optimum component sizing is important in design and integration of solar systems with industrial process applications. In this paper, a methodology is proposed to design and optimize concentrating solar collector based systems with pressurized hot water storage. The proposed methodology is based on the concept of design space. The concept of design space was introduced by Kulkarni et al. (2007) to design and optimize flat plate solar collector based system. However, the proposed methodology is restricted as the storage water temperature is less than 100°C. For medium temperature industrial application, water needs to be pressurized to avoid boiling inside the receiver and storage tank. In this paper, the original concept of design space is extended to include pressurized hot water storage. It may be noted that the proposed methodology has been applied with the assumption of a well mixed storage tank. In reality, there is thermal stratification for large storage tank. Relaxing the assumption of well mixed storage tank and accounting for storage tank stratification will definitely improve the system performance and provide benefit in system sizing. Present research is directed towards

incorporating the effect of thermal stratification on the optimal sizing of the overall system. Design space is the region bounded by constant solar fraction curves traced on the collector area vs. storage volume diagram and it represents all possible feasible design configurations subject to different constraints. Constraints such as existing collector area, limitations on available floor spacing, existing storage volume, or maximum allowable storage volume due to structural restriction, etc. can easily be incorporated in the proposed methodology. The proposed design space approach may be useful in retrofit cases as well. The problem of design and optimization of a real system is usually a multi-objective task. To capture the effects of different objective function, the Pareto optimal region should be identified. The Pareto optimal region signifies the portion of the design space where the optimal solution lies. Depending upon the objective function, an optimal solution from the Pareto optimal region may be selected for sizing the system appropriately. In case of a flat plate solar collector-based system, the Pareto optimal region comprises of the region bounded by the loci of the minimum collector area requirement and the minimum storage volume requirement.

However, this region does not represent a Pareto optimal region for concentrating collector based system. This is because additional variables such as heat exchanger size and the maximum storage temperature also influence the system sizing. Application of the proposed methodology is illustrated through a case study of pasteurization of milk. The thermal demand of the pasteurization process is 1.88 GJ over 4 h a day (45000 l of hot water at 90°C) to pasteurize 30000 l of milk per day. It is observed that the global optimum configuration of the system corresponds to a solar fraction of 0.87. When compared with the existing system, the global optimum design demonstrates a 23% saving in the total annualized cost. Due to uncertainties associated with system parameters, solar isolation, cost data, etc. a globally optimum value may not necessarily provide a meaningful result in actual practice. A range of possible designs with near-minimum total annualized cost is also identified. Based on the actual cash flow, a designer can appropriately design the system. The proposed design and optimization tool offers flexibility to the designer in choosing a system configuration on the basis of desired performance and economy. The design tool makes an attempt, to contribute towards the global endeavor of enhanced and accelerated utilization of solar energy in industrial processes. The study demonstrates the possibility of application of design space methodology to a variety of industrial process heat configurations in an effective way.

References

[1] Abdel-Dayem, A.M., Mohamad, M.A., 2001. Potential of solar energy utilization in the textile industry – a case study. Renewable Energy 23, 685–694.

[2] Brownell, L.E., Young, E.H., 1959. Process Equipment Design. John Wiley, New York, USA. Clark, J.A., 1982. An analysis of the technical and economic performance of a parabolic trough concentrator for solar industrial process heat application. International Journal of Heat and Mass Transfer, 1427– 1438.

[3] Chopey, N.P., 2004. Handbook of Chemical Engineering Calculations, third ed. McGraw Hill, New York, p. 19.37.

[4] Duffie, J.A., Beckman, W.A., 1991. Solar Engineering of Thermal Processes, second ed. John Wiley and Sons, New York, pp. 686–732.

[5] Eskin, N., 2000. Performance analysis of solar process heat system. Energy Conversion and Management 41, 1141–1154.

[6] ESTIF (European Solar Thermal Industry Federation), 2004. A Study on Key Issues for Renewable Heat in Europe(K4RES-H), Solar Industrial Process Heat – WP3, Task 3.5, Contract EIE/04/204nS07.38607.

[7] Gordon, J.M., Rabl, A., 1982. Design analysis and optimization of industrial process heat plants without storage. Solar Energy 28, 519– 530.

[8] Hawlader, M.N.A., Ng, K.C., Chandratilleke, T.T., Sharma, D., Koay, H.L.K., 1987. Economic evaluation of a solar water heating system. Energy Conversion Management 27, 197–204.

[9] ISO 9459–3:1997(E), 1997. Performance Tests for Solar Plus Supplementary Systems. Organization for International Standards, Geneva, Switzerland, p. Kalogirou, S.A., 2003. The potential of industrial process heat applications. Applied Energy 76, 337–361.

[10] Kalogirou, S.A., 2004. Optimization of solar systems using artificial neural networks and genetic algorithms. Applied Energy 77, 383–405.

[11] Klein, S.A., Beckman, W.A., 1979. A general design method for closed loop solar energy systems. Solar Energy 22, 269–282.

[12] Klein, S.A., Beckman, W.A., Duffie, J.A., 1976. A design procedure for solar heating systems. Solar Energy 18, 113–127.

[13] Klein, S.A., Cooper, P.I., Freeman, T.L., Beekman, D.L., Beckman, W.A., Duffie, J.A., 1975. A method of simulation of solar processes and its application. Solar Energy 17, 29–37.

[14] Kedare, S.B., 2006. Solar Concentrator for Industrial Process. In: Sastry, E.V.R., Reddy, D.N. (Eds.), Proceedings of the International Congress on Renewable Energy 2006, Hyderabad (India), pp. 142–147.

[15] Kulkarni, G.N., Kedare, S.B., Bandyopadhyay, S., 2007. Determination of design space and optimization of solar water heating systems. Solar Energy 81 (8), 958–968.

[16] Kulkarni, G.N., 2008. Design and Optimization of solar thermal Systems, Ph.D. Thesis, Indian Institute of Technology, Bombay, India.

[17] Kutscher, C.F., Davenport, R.L., Dougherty, D.A., Gee, R.C., Masterson, M.P., Kenneth, M., 1982. Design Approaches for Solar Industrial Process Heat Systems. Solar Energy Research Institute, USA. Mani, A., 1981. Handbook of Solar Radiation Data for India, first ed. Allied Publishers Pvt Ltd., New Delhi, pp. 381–397.

[18] Michelson, E., 1982. Multivariate optimization of a solar water heating system using the simplex method. Solar Energy 29, 89–99.
[19] PSG, 1993, Design data, Compiled by Faculty of Mechanical Engineering, PSG College of Technology, Coimbatore 641 004, India.
[20] Pareira, M.C., Gordon, J.M., Rabl, A., Zarmi, Y., 1984. Design and optimization of solar industrial hot water systems with storage. Solar Energy 32, 121–133.
[21] Proctor, D., Morse, R.N., 1977. Solar energy for the Australian food processing industry. Solar Energy 19, 63–72.
[22] Shenoy, U.V., Sinha, A., Bandyopadhyay, S., 1998. Multiple utilities targeting for heat exchanger networks. Transactions of IChemE: Chemical Engineering Research and Design 76 (3), 259–272.
[23] Weiss, W., 2003. Solar Heat for Industrial Processes, SHC Annex 33, Solar PACES Annex 4. International Energy Agency, pp. 2–7.

